

# Electron Transport through $\text{YBa}_2\text{Cu}_3\text{O}_{7-\delta}$ Grain Boundary Interfaces between 4.2 and 300 K

C. W. Schneider, S. Hembacher, G. Hammerl, R. Held, A. Schmehl, A. Weber, T. Kopp, and J. Mannhart  
*Experimentalphysik VI, Center for Electronic Correlations and Magnetism, Institute of Physics, Augsburg University,  
D-86135 Augsburg, Germany*

(Received 18 July 2003; published 24 June 2004)

The current-induced dissipation in  $\text{YBa}_2\text{Cu}_3\text{O}_{7-\delta}$  grain boundary tunnel junctions has been measured between 4.2 and 300 K. It is found that the resistance of  $45^\circ(100)/(110)$  junctions decreases linearly by a factor of 4 when their temperature is increased from 100 to 300 K. At the superconducting transition temperature  $T_c$  the grain boundary resistance of the normal state and of the superconducting state extrapolates to the same value.

DOI: 10.1103/PhysRevLett.92.257003

PACS numbers: 74.20.Rp, 74.50.+r, 74.78.Bz, 85.25.Cp

Soon after the discovery of superconductivity in  $\text{La}_{2-x}\text{Ba}_x\text{CuO}_4$  [1] it was realized that the normal-state properties of the high- $T_c$  cuprates differ significantly from those of the low- $T_c$  superconductors. The most prominent and still unexplained normal state properties of the high- $T_c$  compounds are the linear temperature dependence of the in-plane resistivity in the optimally doped compounds [2], spin and charge inhomogeneities [3], and the pseudogap present in the underdoped regime [4].

The complex electronic behavior of the high- $T_c$  materials is also reflected in the characteristics of their interfaces. For  $T < T_c$ , for example, large-angle grain boundaries are excellent tunneling barriers [5], a feature unknown from conventional superconductors. Several mechanisms responsible for the electronic transport properties of grain boundaries and other interfaces have been identified for the temperature range below  $T_c$ , such as the  $d_{x^2-y^2}$  dominated order parameter symmetry, structural effects, and space charge layers [5]. In fact, grain boundaries operated below  $T_c$  have been used to reveal fundamental properties of the high- $T_c$  cuprates, such as the existence of Cooper pairs [6] or the unconventional order parameter symmetry [7].

As is the case for  $T < T_c$ , we expect valuable information on the interfaces of the cuprates, or even on the bulk materials themselves, to be contained in the tunneling characteristics of grain boundaries for  $T > T_c$ . However, only very few data are available for this temperature regime [5,8]. This lack of data arises from the difficulty to measure the grain boundary current-voltage [ $I(V_{gb})$ ] characteristics free of voltages produced by the bridges that are needed to contact the interfaces. By utilizing a difference technique to subtract these unwanted voltages, we have now succeeded in measuring the current-voltage characteristics of  $\text{YBa}_2\text{Cu}_3\text{O}_{7-\delta}$  grain boundaries for  $4.2 \leq T \leq 300$  K. These studies provide evidence that the normal state resistance of  $45^\circ(100)/(110)$  tilt grain boundaries is not influenced by the onset of the superconducting transition. The experiments furthermore reveal that for  $T > T_c$  the resistance of these

grain boundaries decreases linearly with increasing temperature.

The experiments were performed with bicrystalline  $\text{YBa}_2\text{Cu}_3\text{O}_{7-\delta}$  films grown by pulsed laser deposition at  $760^\circ\text{C}$  in 0.25 mbar of  $\text{O}_2$  to a typical thickness of 40–50 nm. The  $\text{SrTiO}_3$  substrates contained symmetric and  $(100)/(110)$  asymmetric  $45^\circ[001]$  tilt grain boundaries, specified to within  $1^\circ$ . After deposition, the samples were cooled during 2 h in an  $\text{O}_2$  pressure of 400 mbar. Because the deposition geometry was tuned to optimize the homogeneity of the samples,  $T_c$  varied by less than 0.5 K across the wafers, while the thickness variations were smaller than 10%. For the four-point measurements, gold contacts were structured photolithographically before the  $\text{YBa}_2\text{Cu}_3\text{O}_{7-\delta}$  films were patterned by etching in a  $\text{H}_3\text{PO}_4$  solution, or by dry etching with an Ar ion beam. The  $\text{YBa}_2\text{Cu}_3\text{O}_{7-\delta}$  bridges had widths and lengths between the voltage probes of  $\approx 2.5$  and  $30 \mu\text{m}$ , respectively (see Fig. 1), and their  $T_c$  varied less than 200 mK. In addition, several samples were patterned into

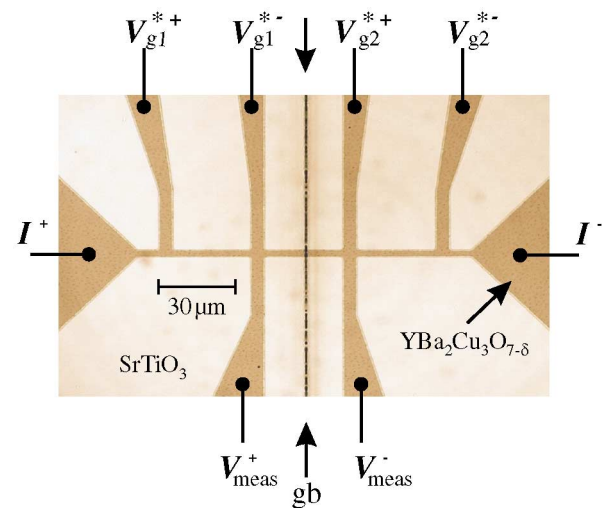


FIG. 1 (color online). Optical micrograph of a three-bridge sample used to measure  $R_{gb}$ . The  $45^\circ$  grain boundary (gb) is indicated by the arrows.

Wheatstone-bridge configurations, of which each arm consists of a meander line containing 23 straight sections with widths of  $\approx 6 \mu\text{m}$ . Two of the meander lines were patterned such that each of the 23 sections crosses the boundary once.

The technique to measure precisely the grain boundary resistance  $R_{\text{gb}}$  below  $T_c$  is based on measuring the  $I(V_{\text{gb}})$  characteristics of the Josephson junctions while applying a microwave field large enough to suppress their critical current. For this purpose, we used low frequency microwaves ( $< 10 \text{ GHz}$ ) to avoid inaccuracies resulting from the Shapiro steps.

All measurements were conducted in shielded rooms using motor-driven dipsticks. The samples were cooled at 4.2 K in liquid Helium, at 77 K in liquid nitrogen, and at other temperatures via He or  $\text{N}_2$  vapor and thermal conduction across the sample holder. Immersion into the cooling liquids did not affect the characteristics, providing evidence that self-heating is insignificant under the experimental conditions.

For  $T > T_c$  the transport properties of the interfaces cannot be measured with a straightforward four-point technique because the voltage  $V_{\text{meas}}$  generated by a bridge straddling the boundary is composed of two contributions: (a) the grain boundary voltage  $V_{\text{gb}}$  and (b) the voltages  $V_{\text{g1}}$  and  $V_{\text{g2}}$  caused by the resistive grains inside the bridge. This problem can be solved by subtracting from  $V_{\text{meas}}$  the grain contributions  $V_{\text{g1}}$  and  $V_{\text{g2}}$ . For this,  $V_{\text{g1}}$  and  $V_{\text{g2}}$  are obtained by approximating them with the voltages  $V_{\text{g1}}^*$  and  $V_{\text{g2}}^*$  generated by independent intragrain bridges that are measured simultaneously. Not surprisingly, test measurements revealed variations of  $V_{\text{g1}}^*$  and  $V_{\text{g2}}^*$  of several percent as a function of the bridge location. Therefore, the intragrain bridges were placed as closely as possible to the boundary bridge (see Fig. 1). The desired measurement accuracy also determined the optimum size of the bridges. On the one hand, the bridges were patterned to be as small as possible so that they could be located close to the grain boundary. On the other hand, their size was chosen to be large enough for the patterning-induced scatter of the bridge aspect ratios to be insignificant. In samples optimized this way, the voltages across the two bridges  $V_{\text{g1}}^*$  and  $V_{\text{g2}}^*$  were identical to within 1% at 100 K and to 0.3% for  $T > 200 \text{ K}$ . Therefore the grain boundary voltage equals with the same accuracy  $V_{\text{gb}} \approx V_{\text{meas}} - (V_{\text{g1}}^* + V_{\text{g2}}^*)/2$ .

As introduced by Mathur *et al.* [9] for studies of  $\text{La}_{1-x}\text{Ca}_x\text{MnO}_3$  bicrystals, and similar to the work described in Ref. [8], we also patterned several samples into Wheatstone bridges. This approach has the advantage that the generated voltages are huge and that  $V_{\text{g1}}^*$  and  $V_{\text{g2}}^*$  are subtracted from  $V_{\text{meas}}$  already during the measurement. Having performed measurements with such bridges, we checked their balance by photolithographically cutting the Wheatstone configurations to individually assess the resistances of the meander lines. Because these studies

revealed  $T$  dependent balancing errors of 1%–10%, we preferred the three-bridge approach for measurements of the  $R_{\text{gb}}(T)$  characteristics, while Wheatstone bridges were chosen when a large signal was required, as was the case for some studies of  $I(V)$  characteristics.

To gain insight into the electronic transport mechanisms, we measured the  $I(V)$  characteristics between 4.2 and 300 K by using Wheatstone bridges. For  $T > T_c$  the characteristics are nonlinear on this large voltage scale, in particular below 150 K (see Fig. 2). Analyzing the nonlinearity, we first note that the microstructure of the grain boundaries is inhomogeneous down to the unit cell level [5]. The  $I(V)$  curves are therefore generated by large numbers of microstructurally different channels connected in parallel. The behavior of the averaged junctions is consistent with the one of a back-to-back Schottky contact as predicted by the band bending model [10]. If tentatively described by a Simmons fit [11], the averaged  $I(V)$  characteristics correspond to heights and widths of hypothetical effective junction barriers of  $\approx 100 \text{ meV}$  and 1–2 nm. Thus, these data suggest unusually small barrier heights. They are, in particular, much smaller than the energy scale of grain boundary built-in potentials measured by electron holography of  $\approx 2 \text{ eV}$  [12].

At small voltages,  $V_{\text{gb}} \approx 10 \text{ mV}$ , the nonlinearity of the  $I(V)$  curves is insignificant, and they are characterized by their Ohmic resistance, which can be obtained by selecting an appropriate voltage ( $V_{\text{cr}}$ ) or current ( $I_{\text{cr}}$ ) criterion  $V_{\text{cr}} = I_{\text{cr}} \times R_{\text{gb}} < 10 \text{ mV}$ . For  $T < T_c$ , due to the microwave irradiation, the  $I(V)$  characteristics are linear, too, even over a larger voltage range. The only exception is given by  $45^\circ$  boundaries at  $T < 40 \text{ K}$ , which will be discussed below. Applying the three-bridge technique, we were therefore able to deduce the  $R_{\text{gb}}(T)$  dependence of a given grain boundary by measuring in one

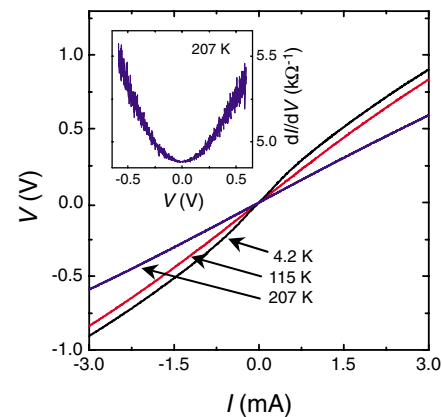


FIG. 2 (color online). Current-voltage characteristics of a Wheatstone bridge containing 23 junctions with a  $45^\circ$  asymmetric boundary in a 50 nm thick  $\text{YBa}_2\text{Cu}_3\text{O}_{7-\delta}$  film. The voltage  $V$  corresponds to the voltage across all junctions,  $V = 23 \times V_{\text{gb}}$ , the current  $I$  is twice the current flowing through one meander line.

temperature sweep from 4.2 to 300 K just one boundary bridge plus the two intragrain reference bridges. Hereby one voltage or current criterion, typically  $I_{cr} = 100 \mu\text{A}$ , is used for all temperatures.

The  $R(T)$  dependence of a  $45^\circ$  symmetric grain boundary measured this way is presented in Fig. 3. The resistance-area product  $R_{gb}A$  (77 K)  $\approx 1 \times 10^{-8} \Omega \text{ cm}^2$  compares well with literature values [5]. Three remarkable features are displayed by the temperature dependence of the resistance. First, the resistance reaches a maximum at  $\approx 30$  K (see also Fig. 4). This maximum is not displayed by symmetric  $24^\circ$  and  $36^\circ$  boundaries measured as reference samples. Second, around  $T_c$  the resistance develops a distinct peak structure. This peak, which is not associated with the microwave irradiation, was found to vary from sample to sample, and to change with time over weeks. Except for this peak, the grain boundary resistance of the normal state and of the superconducting state extrapolate within the measurement accuracy of  $\approx 2\%$  to the same value  $R_{gb}(T_c) = 10.7 \Omega$ . This temperature dependence is characteristic for all samples we have studied, except for few that displayed at  $T_c$  a resistance step of  $\leq 5\%$ . As this step was found to be not reproducible and to increase for a given sample over weeks, we consider it to be an artifact resulting from chemical reactions or diffusion. Third, between 100 and 300 K the resistance decreases with increasing temperature by a factor of 4. The temperature dependence is hereby remarkably linear, with a barely noticeable positive curvature (Fig. 3, upper inset). This is in striking contrast to the linear resistance increase of the adjacent  $\text{YBa}_2\text{Cu}_3\text{O}_{7-\delta}$  grains (Fig. 3, lower inset). In the following, we will discuss the three features and their implications for the understanding of the interfaces, beginning with the superconducting regime.

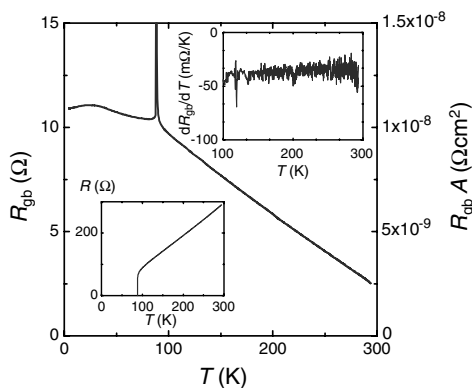


FIG. 3. Measured temperature dependence of the resistance of a  $45^\circ$  symmetric grain boundary in a 40 nm thick  $\text{YBa}_2\text{Cu}_3\text{O}_{7-\delta}$  film ( $I_{cr} = 100 \mu\text{A}$ ). The peak reaches a maximum of  $25 \Omega$  at 88.3 K. The insets show  $dR/dT(T)$  for the grain boundary and the corresponding  $R(T)$  curve of one grain located next to the boundary.

At low temperatures, the resistance of  $45^\circ$  grain boundaries changes nonmonotonically with  $T$ , and even depends on the value of the tunneling current (see Fig. 4). This maximum and its current bias dependence are consistent with the formation of a zero-bias anomaly by the faceted  $45^\circ$  junctions. At small bias currents  $V_{gb}$  is of the order of 1 mV, and therefore sufficiently small to probe the temperature dependent shape of the zero-bias conductance peak in the superconducting energy gap. This zero-bias conductance peak is usually presumed to arise from Andreev bound states generated by the  $d_{x^2-y^2}$  order parameter symmetry of  $\text{YBa}_2\text{Cu}_3\text{O}_{7-\delta}$  [13].

The peak structure at 89 K provides evidence that at  $T_c$  the resistance of the grain boundary bridge is much larger than the resistance of the intragrain bridges. The observed height of the peak shown in Fig. 3 is consistent with a  $T_c$  difference of the bridges of 150 mK. The shape of the peak is influenced by the differences in the fluctuations of the intragrain bridges and the one containing the tunnel junction. Unfortunately we cannot extract data on this effect from the peak, as the spatial distribution of  $T_c$  is unknown.

The grain boundary resistance values above and below  $T_c$  extrapolate to the same value at the transition temperature. The transition into the superconducting state is therefore found not to affect the dissipation in the junctions at  $T_c$ . This observation cannot be reconciled with the predictions for surface charging effects in the hole superconductivity scenario introduced by Hirsch and Marsiglio [14]. In this scenario, charges are separated in the superconducting state in the vicinity of a grain boundary, but not above  $T_c$ . This charge separation is expected to change the electronic properties of the interfaces when passing through  $T_c$  [15]. The grain boundary data do not show this effect.

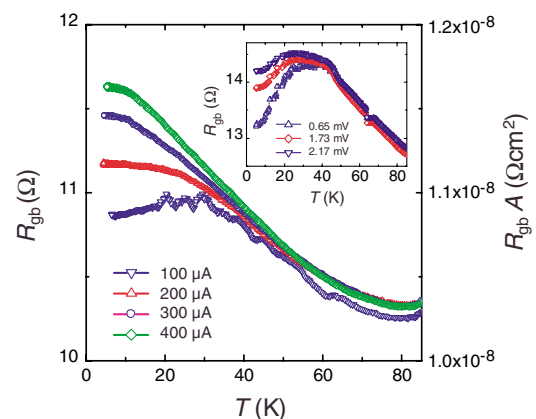


FIG. 4 (color online). Temperature dependence of the resistance of a  $45^\circ$  symmetric grain boundary in a 40 nm thick  $\text{YBa}_2\text{Cu}_3\text{O}_{7-\delta}$  film measured in the three-bridge configuration. The inset shows the temperature dependent resistance of a  $45^\circ$  asymmetric grain boundary in a 50 nm thick film measured in a Wheatstone-bridge configuration.

For  $T > T_c$ , the grain boundary resistance decreases linearly. This behavior cannot be explained by elastic tunneling from the vicinity of a well-defined Fermi surface across standard Schottky contacts with  $T$ -independent barrier heights and widths [16]. There, a nonlinear and weak  $R_{gb}(T)$  characteristic is expected for the parameter range derived above. A more detailed elastic tunneling model has to include  $T$ -dependent Schottky barriers and to consider the spatial inhomogeneity of the interface. To significantly alter the weak and nonlinear  $T$  dependence both effects demand the thermal energy  $k_B T$  to exceed the energy scales of the barrier for large parts of the interface areas. Hereby a very special energy profile of the barriers is required to yield the linear  $R_{gb}(T)$  behavior over a large temperature range. This situation seems unphysical to us. We note that inelastic tunneling via resonant impurity channels [17] cannot account for the linear temperature characteristic either. Considering the problems which standard semiconductor models have in describing the observed interface characteristics, we now turn our attention to the effect of the electronic correlations present in the cuprates.

As pointed out by Miller and Freericks [18], electronic correlations strongly affect the barrier properties of high- $T_c$  interfaces in the superconducting state. This is also true in the normal conducting state. As suggested by the band bending model [10], the barrier is an underdoped region, with the possible formation of antiferromagnetic fluctuations or even of local magnetic moments. The resultant magnetic scattering is expected to increase the interface resistance with decreasing temperature. Since the density of the magnetic moments is not known, the  $R_{gb}(T)$  dependence cannot be determined yet. Besides correlations in the barrier, electronic correlations in the bulk may also influence the transport through the interface. What would be expected if, due to the grain boundary charging, the  $\text{YBa}_2\text{Cu}_3\text{O}_{7-\delta}$  layers adjacent to the grain boundary were underdoped, characterized by a pseudogap and, possibly, by preformed pairs? The spectral densities of the electronic excitations on both sides of the interface control the tunneling process. It is only for the  $45^\circ$  grain boundaries under consideration that the nodal and antinodal directions of the pseudogap are directly coupled, and the tunneling current is most strongly reduced. As the pseudogap diminishes for increasing temperature, the boundary conductivity is expected to increase. Here we note that the  $R_{gb}(T)$  curve is

characterized by one temperature scale,  $T_0$ , the extrapolated zero-resistance intercept. In the samples investigated,  $T_0 \approx 350$  K, which corresponds to the pseudogap energy scale of underdoped  $\text{YBa}_2\text{Cu}_3\text{O}_{7-\delta}$ .

In summary, it is found that the resistance of  $45^\circ[001]$  tilt  $\text{YBa}_2\text{Cu}_3\text{O}_{7-\delta}$  grain boundary junctions decreases linearly with increasing temperature for  $T > T_c$ . In the vicinity of  $T_c$  the grain boundary resistance and thus the dissipation are indistinguishable for  $T < T_c$  and  $T > T_c$ , in contradiction to predictions of the theory of hole superconductivity. The  $I(V)$  characteristics between 4.2 and 300 K are nonlinear, suggesting a tunneling barrier with an effective height and width of  $\approx 0.1$  eV and  $\approx 1-2$  nm, respectively. The linear  $R_{gb}(T)$  dependence is proposed to be caused by correlation controlled tunneling.

The authors gratefully acknowledge helpful discussions with Y. Barash, H. Bielefeldt, M. Blamire, U. Eckern, P.J. Hirschfeld, C. Laschinger, J. Ransley, A. Rosch, D.G. Schlom, and M. Siegel. This work was supported by the DFG through the SFB 484 and by the BMBF via Project No. 13N6918A.

- 
- [1] J.G. Bednorz and K. A. Müller, *Z. Phys. B* **64**, 189 (1986).
  - [2] S.W. Tozer *et al.*, *Phys. Rev. Lett.* **59**, 1768 (1987).
  - [3] J. Orenstein and A. J. Millis, *Science* **288**, 468 (2000).
  - [4] T. Timusk and B. Statt, *Rep. Prog. Phys.* **62**, 61 (1999).
  - [5] H. Hilgenkamp and J. Mannhart, *Rev. Mod. Phys.* **74**, 485 (2002).
  - [6] C. E. Gough *et al.*, *Nature (London)* **326**, 855 (1987).
  - [7] C. C. Tsuei and J. R. Kirtley, *Rev. Mod. Phys.* **72**, 969 (2000).
  - [8] J. H. T. Ransley *et al.*, *IEEE Trans. Appl. Supercond.* **13**, 2886 (2003).
  - [9] N. D. Mathur *et al.*, *Nature (London)* **387**, 266 (1997).
  - [10] J. Mannhart and H. Hilgenkamp, *Mater. Sci. Eng. B* **56**, 77 (1998).
  - [11] J.G. Simmons, *J. Appl. Phys.* **34**, 1828 (1963).
  - [12] M. A. Schofield *et al.*, *Phys. Rev. B* **67**, 224512 (2003).
  - [13] C.-R. Hu, *Phys. Rev. Lett.* **72**, 1526 (1994).
  - [14] J. Hirsch and F. Marsiglio, *Phys. Rev. B* **39**, 11515 (1989).
  - [15] J. Hirsch, *Phys. Lett. A* **281**, 44 (2001).
  - [16] E. L. Wolf, *Principles of Electron Tunneling Spectroscopy* (Clarendon, Oxford, 1985).
  - [17] L. I. Glazman and K. A. Matveev, *Sov. Phys. JETP* **67**, 1276 (1988); **49**, 659 (1989).
  - [18] P. Miller and J. K. Freericks, *J. Phys. Condens. Matter* **13**, 3187 (2001).